ISSN 0021-3640, JETP Letters, 2016, Vol. 103, No. 4, pp. 254–259. © Pleiades Publishing, Inc., 2016.
Original Russian Text © V.G. Myagkov, L.E. Bykova, V.Yu. Yakovchuk, V.S. Zhigalov, M.N. Volochaev, A.A. Matsynin, I.A. Tambasov, V.A. Seredkin, G.S. Patrin, G.N. Bondarenko, 2016, published in Pis'ma v Zhurnal Eksperimental'noi i Teoreticheskoi Fiziki, 2016, Vol. 103, No. 4, pp. 280–285.

CONDENSED MATTER

Structural and Magnetic Features of Solid-Phase Transformations in Mn/Bi and Bi/Mn Films

V. G. Myagkov[a], L. E. Bykova[a], V. Yu. Yakovchuk[a], V. S. Zhigalov[a, b], M. N. Volochaev[a, b], A. A. Matsynin[a], I. A. Tambasov[a], V. A. Seredkin[a], G. S. Patrin[a, c], and G. N. Bondarenko[d]

[a] *Kirensky Institute of Physics, Siberian Branch, Russian Academy of Sciences, Akademgorodok, Krasnoyarsk, 660036 Russia*

[b] *Siberian State Aerospace University, pr. Gazety Krasnoyarskii Rabochii, Krasnoyarsk, 660014 Russia*

[c] *Institute of Chemistry and Chemical Technology, Siberian Branch, Russian Academy of Sciences, Krasnoyarsk, 660036 Russia*

[d] *Siberian Federal University, Svobodnyi pr. 79, Krasnoyarsk, 660041 Russia*

e-mail: miagkov@iph.krasn.ru

Received December 28, 2015

Solid-phase transformations at different annealing temperatures in Mn/Bi (Mn on Bi) and Bi/Mn (Bi on Mn) films have been studied using X-ray diffraction, electron microscopy, and magnetic measurements. It has been shown that the synthesis of the α-MnBi phase in polycrystalline Mn/Bi films begins at a temperature of ~120°C and the Mn and Bi layers react completely at 300°C. The resulting α-MnBi(001) samples have a large perpendicular magnetic anisotropy ($K_u \simeq 1.5 \times 10^7$ erg/cm^3) and a coercive force $H > H_C \sim 3$ kOe. In contrast to Mn/Bi, the ferromagnetic α-MnBi phase in Bi/Mn films is not formed even at annealing processes up to 400°C and Mn clusters are formed in a Bi melt. This asymmetry in phase transformations occurs because chemosorbed oxygen existing on the surface of the Mn film in Bi/Mn films suppresses a solid-phase reaction between Mn and Bi. The analysis of the results obtained implies the existence of new low-temperature (~120°C) structural transformation in the Mn–Bi system.

DOI: 10.1134/S0021364016040111

INTRODUCTION

The MnBi intermetallic compound has many unique magnetic and structural properties and is considered as a possible alternative to rare-earth and expensive magnets [1]. The low-temperature ferromagnetic phase LTP-MnBi (α-MnBi) with the NiAs structure has a large uniaxial anisotropy ($K_u \simeq 1.5 \times 10^7$ erg/cm^3) with the c easy axis and the saturation magnetization at room temperature is M_S = 712 emu/cm^3 [2]. An increase in the temperature above 663 K is accompanied by the structural transition of the α-MnBi phase to the high-temperature paramagnetic phase HTP-MnBi (β-MnBi) with the distorted Ni_2In structure with $Mn_{1.08}Bi$ stoichiometry. This transition is attributed to the peritectic decomposition of the α-MnBi phase to the $Mn_{1.08}Bi$ and Bi phases [3–5]:

$$\alpha \rightarrow \beta + \text{Bi}. \quad (1)$$

The fast cooling of the HTP-MnBi phase to low temperatures results in the formation of the so-called ferrimagnetic rapidly quenched high-temperature phase QHTP-MnBi (quenched HTP-MnBi) without a change in the orthorhombic structure and composition. The metastable phase QHTP-$Mn_{1.08}Bi$ has the Curie temperature of ≃440 K and the magnetic anisotropy constant $K_u = 3.0 \times 10^7$ erg/cm^3 larger than that for the LTP-MnBi phase and M_S = 480 emu/cm^3 at room temperature [3]. Thermal instability and high sensitivity to oxidation are negative properties for applications of QHTP-MnBi compounds. Significant efforts were applied to stabilize and improve the structural and magnetic properties of the QHTP-MnBi phase by doping it with a third element [6, 7]. It is assumed that the QHTP-$Mn_{1.08}Bi$ phase is unstable at room temperature and is transformed in two years to the stable α-MnBi phase through the reaction [4]

$$\text{QHTP-Mn}_{1.08}\text{Bi} \rightarrow \alpha\text{-MnBi} + \text{Mn}. \quad (2)$$

However, Hauder and Unger [8] showed that the QHTP-$Mn_{1.08}Bi$ phase is transformed to the α-MnBi phase through the new third indefinite metastable phase in the temperature range between 80°C and 220°C and above 95°C in $Mn_{1-x}Ti_xBi$ films [9]. Although the high-temperature part of the diagram of Mn–Bi was supplemented [5], the above results and

the formation of metastable and quasicrystalline phases [10, 11] imply that the low-temperature part of the phase diagram of Mn–Bi was poorly determined. In many works, highly anisotropic MnBi films were obtained through solid-phase reactions between Mn and Bi layers [2–4, 7, 11, 12]. Chemical interactions between Mn, Bi, and O, which strongly affect the formation of ferromagnetic phases in the Mn–Bi system were studied only in a few works.

SAMPLES AND EXPERIMENTAL PROCEDURE

The experiments were performed with Mn/Bi and Bi/Mn films obtained by the successive thermal deposition of Mn on Bi and Bi on Mn on glass and pyroceram substrates in a vacuum of 10^{-6} Torr. The deposition of Mn and Bi layers with approximate stoichiometry Mn : Bi = 1 : 1 and a total thickness of 350 nm was performed at a temperature below 100°C. The initial Mn/Bi and Bi/Mn samples were annealed in a vacuum of 10^{-6} Torr from 50 to 300°C with a step of 50°C with aging for 30 min at each temperature. The formed phases were identified on a DRON-4-07 diffractometer in Cu K_α radiation. The samples for transmission electron microscopy were prepared by the cross-section method with the use of a focused ion beam system (FIB, Hitachi FB2100). The electron microscopy studies were performed on a Hitachi HT7700 transmission electron microscope (at 100 kV, W source) equipped with a scanning transmission electron microscopy system (the diameter of the electron probe is 30 nm) and with an energy dispersion X-ray spectrometer (Bruker Nano XFlash 6T/60). The saturation magnetization M_S and perpendicular anisotropy field $H_K = 2K_\perp/M_S$ were determined by the torsional moment method through the procedure proposed in [13]. Magneto-optical hysteresis loops of Faraday rotation were measured at a wavelength of 630 nm in magnetic fields up to 14 kOe. The electric resistance $R(T)$ as a function of the temperature T was measured by the standard four-terminal method in a vacuum of 10^{-6} Torr. The magnetoresistance was measured by the standard four-terminal method in magnetic fields up to 4.5 kOe at room temperature.

EXPERIMENTAL RESULTS

Figure 1 shows the (a) electric resistance $R(T)$ and (b) saturation magnetization $M_S(T)$ of the Mn/Bi (Mn on Bi) sample as function of the annealing temperature T. As the temperature increases, the resistance decreases insignificantly and drops sharply above $T_{in} \sim$ 120°C (Fig. 1b). The samples were nonmagnetic up to the temperature T_{in}, and the magnetization appeared in them at temperatures above T_{in}, increased abruptly at heating to a temperature of 250°C, and varied insignificantly at 300°C (Fig. 1b). After annealing processes at 250 and 300°C, the coercive force of the samples measured perpendicularly to the plane of the film was $H_C \sim 3.1$ kOe (left inset in Fig. 1b). This indicates the beginning of strong mixing of the Mn and Bi layers above the initiation temperature $T_{in} \sim$ 120°C and the formation of the magnetically hard phase α-MnBi, which was completely synthesized at 300°C.

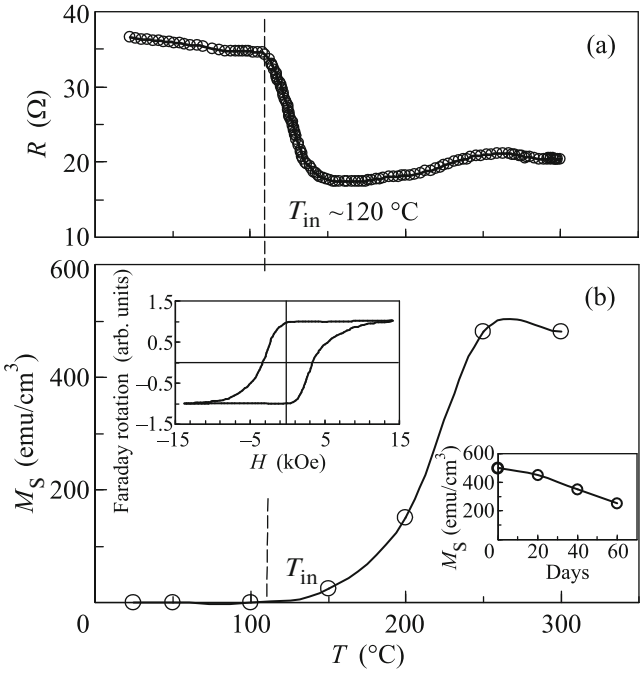

Fig. 1. (a) Electrical resistance R and (b) saturation magnetization M_S of the Mn/Bi (Mn on Bi) sample versus the annealing temperature T. The dashed vertical straight line indicates the temperature of initiation $T_{in} \sim$ 120°C of the magnetically hard α-MnBi phase. The left inset shows the hysteresis loop of the angle of Faraday rotation in the magnetic field perpendicular to the plane of the α-MnBi film obtained after annealing at 300°C. The right inset shows the saturation magnetization M_S versus the time of aging in air of the α-MnBi sample.

The diffraction patterns of the initial bilayer Mn/Bi (Mn on Bi) films contain strong reflections from the Bi(003) and Bi(006) planes and weak reflections from other Bi planes and α-Mn (Fig. 2a), which implies the predominant growth of Bi crystallites with the c axis perpendicular to the substrate and the growth of fine α-Mn grains. After annealing at 150°C, reflections from Bi decreased and reflections from Mn disappeared completely (Fig. 2b), indicating the solid-phase reaction of Mn with Bi. After annealing at 200°C, α-MnBi peaks appeared (Fig. 2c) and became the main peaks after annealing processes at 250°C (Fig. 2d) and 300°C (Fig. 2e). Strong α-MnBi(002) and α-MnBi(004) peaks and the absence of reflections from other phases indicate the complete mixing of the Mn and Bi layers after annealing at 300°C and the predominant synthesis of α-MnBi(001) crystallites on glass substrates. This result agrees well with

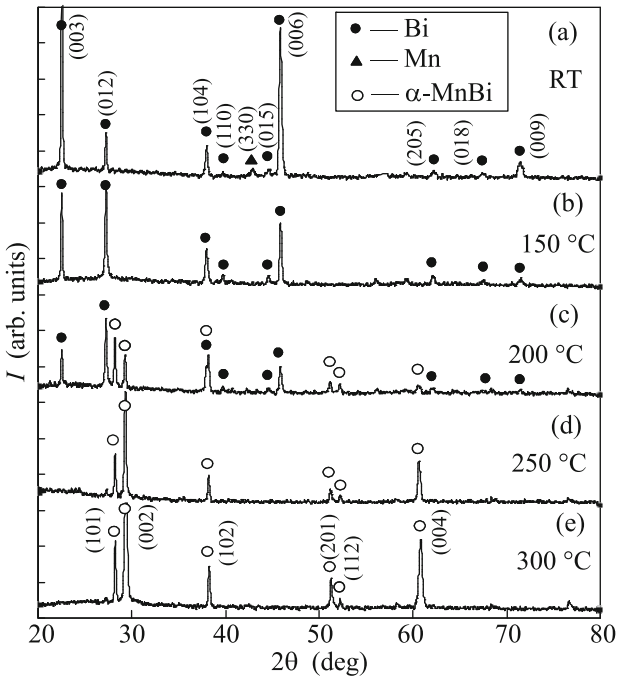

Fig. 2. Diffraction patterns demonstrating phase transformations in the Mn/Bi (Mn on Bi) sample at various annealing temperatures.

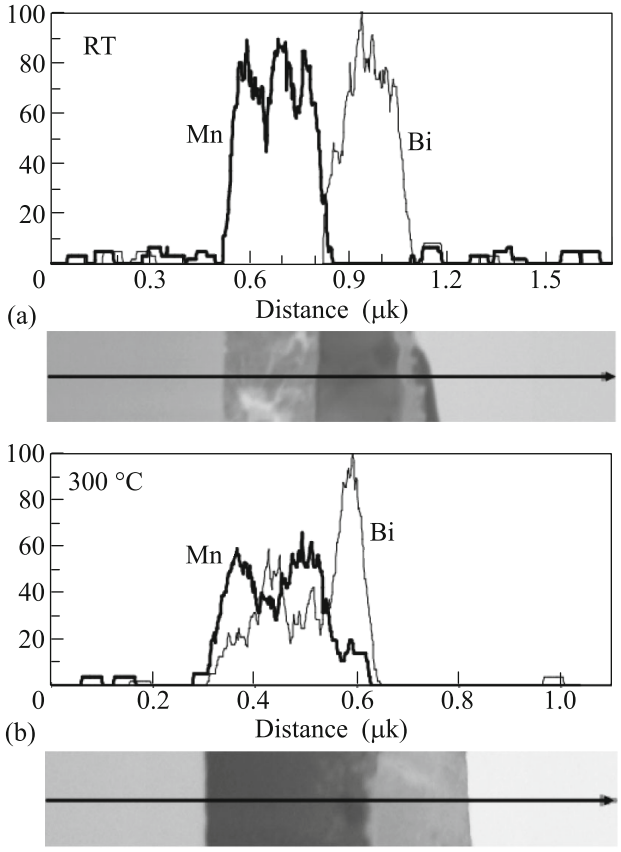

Fig. 3. Transmission electron microscopy image and linear energy dispersion X-ray scans (along the black line) of the cross section of (a) the initial Mn/Bi (Mn on Bi) sample and (b) the sample after annealing at 300°C.

studies on a torque-coil magnetometer, which showed that the α-MnBi samples after annealing processes at 200, 250, and 300°C had an easy axis perpendicular to the plane of the substrate. The saturation magnetization M_S and the perpendicular anisotropy field $H_K = 2K_u/M_S$ (where $K_u = K_1 - 2\pi M_S^2$, K_1 is the first constant of magnetocrystalline anisotropy of the α-MnBi phase, and $2\pi M_S^2$ is the anisotropy of the shape of the film) after annealing processes at 250 and 300°C were $M_S = 500$ emu/cm^3 and $H_K = (60 \pm 5)$ kOe ($K_u = 1.5 \times 10^7$ erg/cm^3). These samples had a low negative magnetoresistance whose magnitude at liquid nitrogen temperature did not exceed ~0.2% in a magnetic field of 4.5 kOe. The saturation magnetization M_S decreased with time, indicating a low chemical stability at aging in air (Fig. 1b).

Electron microscopy studies and linear energy dispersion X-ray scans through the thickness confirm that the initial Mn/Bi films contained Mn and Bi layers (Fig. 3a), which were completely mixed after annealing at 300°C (Fig. 3b). The energy dispersion analysis gives the average value of the atomic concentrations of Mn and Bi, which correspond to the stoichiometry of the α-MnBi phase.

In contrast to the Mn/Bi (Mn on Bi) samples, the Bi/Mn (Bi on Mn) films, in which Mn is deposited as the first layer, after a series of annealing processes up to 400°C remained nonmagnetic or had a very small magnetization. This property indicates that the solid-phase synthesis of the α-MnBi and QHTP-$Mn_{1.08}Bi$ ferromagnetic phases strongly depends on the sequence of deposition of Mn and Bi layers.

The diffraction patterns of the initial Bi/Mn films contained reflections from polycrystalline Bi and from Mn. This implies that a Mn layer grew in a fine-grained form on the glass substrate (Fig. 4a). In addition to reflections from Bi, the diffraction patterns contained peaks that can be attributed to β-Bi_2O_3 oxide metastable at room temperature. The initial Bi/Mn samples also can contain α-Bi_2O_3 oxide because it has common reflections with β-Bi_2O_3 oxide. It is known that the metastable β-Bi_2O_3 and stable α-Bi_2O_3 phases often appear on the Bi surface at low temperatures and remain stable at room temperature [14].

Diffraction patterns after annealing processes at 300 and 400°C contained only reflections from polycrystalline Bi and weak peaks from MnO oxide (Fig. 4b). Figure 5a shows the transmission electron microscopy image of the cross section and composition profiles. Figure 5b presents the composition images of Mn and Bi for the Bi/Mn sample after

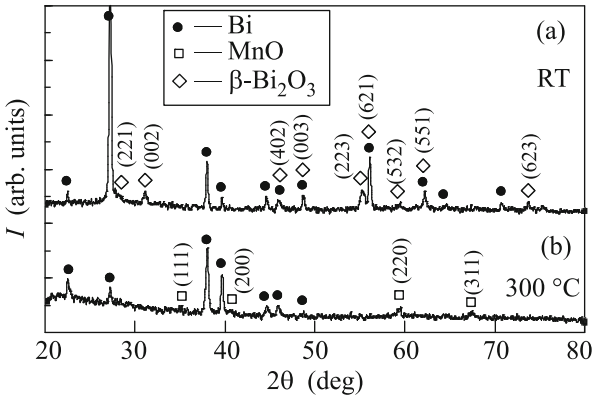

Fig. 4. Diffraction patterns demonstrating phase transformations in the Bi/Mn (Bi on Mn) sample at various annealing temperatures.

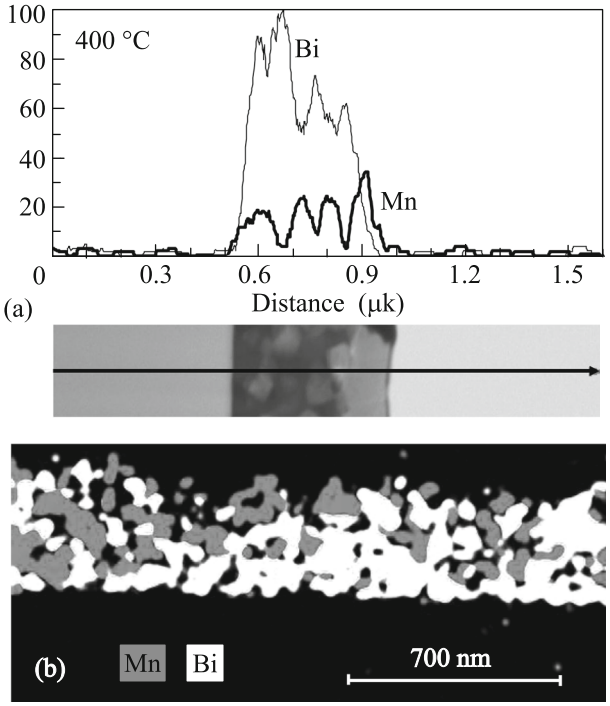

Fig. 5. (a) Transmission electron microscopy image and linear energy dispersion X-ray scans across the Bi/Mn (Bi on Mn) sample (along the black line) after annealing at 400°C. (b) Maps of the elemental composition of the cross section for the Bi/Mn (Bi on Mn) sample after annealing at 400°C.

annealing at 400°C. The in-depth analysis reveals the mixing of Mn and Bi layers without the formation of a homogeneous α-MnBi layer, as occurs under the same annealing conditions in Mn/Bi (Mn on Bi) films, where Bi is deposited as the first layer on the substrate. The possible explanation of various scenarios of phase transformations on interfaces in Mn/Bi and Bi/Mn film systems is that, because of the high reaction capability of Mn, a chemisorbed oxygen layer appears on the surface of Mn deposited as the first layer even in a vacuum of 10^{-6} Torr. The deposition of Bi is accompanied by its reaction with surface oxygen with the formation of Bi_2O_3, which has a large negative formation enthalpy $\Delta H_f = -573.9$ kJ/mol. For this reason, in Bi/Mn samples, where Mn forms the first layer, the formed buffer Bi_2O_3 layer suppresses the reaction between Bi and Mn. When the annealing temperature exceeds the melting temperature of Bi (271.4°C), the Bi layer begins to be melted and to propagate through defects and grain boundaries in the Mn layer, forming Mn clusters with the buffer Bi_2O_3 layer in the bismuth melt. The solid-phase synthesis of α-MnBi occurred in most works when the first layer was Bi [2–4, 7, 12]. However, when the first layer was Mn, the synthesis of α-MnBi occurred only at 300°C in three days [15] or was associated with the formation of a nonmagnetic phase [11]. Asymmetry in chemical mixing at the interface depending on the sequence of deposited layers was experimentally observed and was confirmed by molecular dynamics calculations for certain film systems [16]. These studies revealed mixing through the thickness of several nanometers. The explanation of asymmetric mixing implies the local acceleration of a deposited atom at the interface to a kinetic energy exceeding the energy barrier for atomic mixing [16]. Our studies suggest the decisive role of oxygen pollution in the asymmetry of solid-phase transformations in Mn/Bi and Bi/Mn films and in the degradation of the saturation magnetization at aging of α-MnBi samples in air (right inset in Fig. 1b).

It is well known that solid-phase reactions are characterized by the first forming phase and its initiation temperature T_{in} [17]. It was shown that the initiation temperature T_{in} for many binary systems in bilayer films coincides within the experimental accuracy with the temperatures of solid-phase transformations T_K ($T_{in} = T_K$). The equality $T_{in} = T_K$ is valid for order–disorder phase transitions in Au–Cu (240°C) [18], Fe–Pd (450°C) [19], and Co–Pt (450°C) [20]; for a eutectoid decomposition in Fe–Ni (350°C) [21] and Fe–Cu (850°C) [22]; for martensitic transformations in Al–Ni (180°C) [23], Ti–Ni (850°C) [24], and Au–Cd (60°C) [25]; and for other phase transformations [26]. Consequently, low-temperature solid-phase reactions in thin films occur only in binary systems exhibiting low-temperature solid-phase transformations. The same chemical interactions are responsible for solid-phase reactions in thin films and respective solid-phase transformations. Our studies show that the initiation temperature of the first phase α-MnBi is ~120°C (Fig. 1). This fact implies the existence of a new low-temperature (~120°C) structural transformation in the Mn–Bi system involving the α-MnBi phase. It was shown in the Introduction that such a transformation at low temperatures can be the phase decomposition of the QHTP-$Mn_{1.08}Bi$ phase into the α-MnBi phase according to reaction (2). It is note-

worthy that intensive studies of ferromagnetism in diluted $Mn_{1-x}Ge_x$ ($x > 0.95$) solid solutions revealed a low-temperature ($T_K \sim 120$°C) spinodal decomposition in the Mn–Ge system [27]. It was shown in [28] that the solid-phase reaction in Mn/Ge films begins at the temperature of spinodal decomposition $T_{in} = T_K \sim 120$°C.

CONCLUSIONS

The asymmetry of phase transformations in Mn/Bi (Mn on Bi) and Bi/Mn (Bi on Mn) films near the equiatomic composition has been studied with an increase in the annealing temperature to 300°C. When a Mn layer is deposited on a Bi layer, the reaction begins at a temperature of ~120°C and completely ends at 300°C with the formation of the magnetically hard α-MnBi phase. The deposition of Bi on a Mn layer under the same technological conditions does not lead to a reaction between Mn and Bi at annealing temperatures up to 400°C. The observed asymmetry has been explained under the assumption of the formation of chemisorbed oxygen on the Mn surface; this oxygen reacts with Bi atoms, forming a buffer Bi_2O_3 layer, which suppresses the reaction of Mn with Bi. The analysis of solid-phase reactions in layer film structures implies a solid-phase transformation in the Mn–Bi system at ~120°C.

This work was supported by the Russian Foundation for Basic Research (project nos. 15-02-00948 and 16-03-00069), by the Council of the President of the Russian Federation for Support of Young Scientists and Leading Scientific Schools (project no. SP-317.2015.1), and by the Foundation for Promotion of the Development of Small Scientific and Engineering Enterprises (project nos. 0011727 and 6662GU2015, program Umnik). The electron microscopy studies were performed on the equipment of the Shared Usage Center, Krasnoyarsk Research Center, Siberian Branch, Russian Academy of Sciences.

REFERENCES

1. R. W. McCallum, L. H. Lewis, R. Skomski, M. J. Kramer, and I. E. Anderson, Ann. Rev. Mater. Res. **44**, 10.1 (2014), V. Ly, X. Wu, L. Smillie, T. Shoji, A. Kato, A. Manabe, and K. Suzuki, J. Alloys Compd. **615**, S285 (2014), V. V. Nguyen, N. Poudyal, X. B. Liu, J. P. Liu, K. Sun, M. J. Kramer, and J. Cui, Mater. Res. Express **1**, 036108 (2014), Y.-C. Chen, G. Gregori, A. Leineweber, F. Qu, C.-C. Chen, T. Tietze, H. Kronmüller, G. Schütz, and E. Goering, Scripta Mater. **107**, 131 (2015).
2. P. Kharel, R. Skomski, P. Lukashev, R. Sabirianov, and D. J. Sellmyer, Phys. Rev. B **84**, 014431 (2011).
3. T. Chen and W. E. Stutius, IEEE Trans. Magn. **10**, 581 (1974).
4. D. Chen, J. Appl. Phys. **42**, 3625 (1971).
5. T. Chen, J. Appl. Phys. **45**, 2358 (1974).
6. E. S. Olivetti, C. Curcio, L. Martino, M. Küpferling, and V. Basso, J. Alloys Compd. **643**, S270 (2015), V. Taufour, S. Thimmaiah, S. March, S. Saunders, K. Sun, T. N. Lamichhane, M. J. Kramer, S. L. Bud'ko, and P. C. Canfield, Phys. Rev. Appl. **4**, 014021 (2015).
7. P. Kharel, V. R. Shah, X. Z. Li, W. Y. Zhang, R. Skomski, J. E. Shield, and D. J. Sellmyer, J. Phys. D: Appl. Phys. **46**, 095003 (2013).
8. H. Hauder and W. K. Unger, Phys. Status Solidi A **7**, 393 (1971).
9. W. K. Unger, E. Wolfgang, H. Harms, and H. Haudek, J. Appl. Phys. **43**, 2875 (1972).
10. K. Yoshida and T. Yamada, Appl. Surf. Sci. **33–34**, 516 (1988), K. Yoshida and T. Yamada, Appl. Surf. Sci. **60–61**, 391 (1992), J. Reyes-Gasga, R. Hernández, and M. José-Yacamán, Thin Solid Films **196**, L5 (1991).
11. Y. Iwama and Y. Takeno, Phys. Status Solidi A **76**, 75 (1983).
12. T. Hozumi, P. LeClair, G. Mankey, C. Mewes, H. Sepehri-Amin, K. Hono, and T. Suzuki, J. Appl. Phys. **115**, 17A737 (2014), W. Zhang, P. Kharel, S. Valloppilly, L. Yue, and D. J. Sellmyer, Phys. Status Solidi A **252**, 1934 (2015).
13. S. Chikazumi, J. Appl. Phys. **32**, S81 (1961).
14. J. A. Steele and R. A. Lewis, Opt. Mater. Express **4**, 2133 (2014).
15. H. J. Williams, R. C. Sherwood, and O. L. Boothby, J. Appl. Phys. **28**, 445 (1957).
16. P. Süle, D. Kaptás, L. Bujdoso, Z. E. Horváth, A. Nakanishi, and J. Balogh, J. Appl. Phys. **118**, 135305 (2015), W. Priyantha, R. J. Smith, H. Chen, M. Kopczyk, M. Lerch, C. Key, P. Nachimuthu, and W. Jiang, J. Appl. Phys. **105**, 053504 (2009), S.-P. Kim, S.-C. Lee, K.-R. Lee, and Y.-C. Chung, Acta Mater. **56**, 1011 (2008), S.-G. Lee and Y.-C. Chung, J. Appl. Phys. **105**, 034902 (2009).
17. *Thin Films: Interdiffusion and Reaction*, Ed. by J. M. Poate, K. N. Tu, and J. W. Mayer (Willey-Interscience, New York, 1978); E. G. Colgan, Mater. Sci. Rep. **5**, 1 (1990), R. Pretorius, C. C. Theron, A. Vantomme, and J. W. Mayer, Crit. Rev. Solid State Mater. Sci. **24**, 1 (1999).
18. V. G. Myagkov, L. E. Bykova, V. S. Zhigalov, A. I. Pol'skii, and F. V. Myagkov, JETP Lett. **71**, 183 (2000), V. G. Myagkov, Yu. L. Mikhlin, L. E. Bykova, V. K. Mal'tsev, and G. N. Bondarenko, JETP Lett. **90**, 111 (2009).
19. V. G. Myagkov, V. S. Zhigalov, L. E. Bykova, L. A. Solov'ev, and G. N. Bondarenko, JETP Lett. **91**, 481 (2010), V. G. Myagkov, V. S. Zhigalov, B. A. Belyaev, L. E. Bykova, L. A. Solovyov, and G. N. Bondarenko, J. Magn. Magn. Mater. **324**, 1571 (2012).
20. V. G. Myagkov, L. A. Li, L. E. Bykova, I. A. Turpanov, P. D. Kim, G. V. Bondarenko, and G. N. Bondarenko, Phys. Solid State **42**, 968 (2000).
21. V. G. Myagkov, V. C. Zhigalov, L. E. Bykova, and G. N. Bondarenko, J. Magn. Magn. Mater. **305**, 334 (2006), V. G. Myagkov, V. C. Zhigalov, L. E. Bykova, G. V. Bondarenko, and G. N. Bondarenko, J. Magn. Magn. Mater. **310**, 126 (2007).

22. V. G. Myagkov, O. A. Bayukov, L. E. Bykova, and G. N. Bondarenko, J. Magn. Magn. Mater. **321**, 2260 (2009).

23. V. G. Myagkov and L. E. Bykova, Dokl. Phys. **49**, 289 (2004), V. G. Myagkov, L. E. Bykova, S. M. Zharkov, and G. V. Bondarenko, Solid State Phenom. **138**, 377 (2008).

24. V. G. Myagkov, L. E. Bykova, L. A. Li, I. A. Turpanov, and G. N. Bondarenko, Dokl. Phys. **47**, 95 (2002).

25. V. G. Myagkov, L. E. Bykova, and G. N. Bondarenko, Dokl. Phys. **48**, 30 (2003).

26. V. S. Zhigalov, V. G. Myagkov, L. A. Solov'ev, G. N. Bondarenko, and L. E. Bykova, JETP Lett. **88**, 389 (2008), V. G. Myagkov, L. E. Bykova, G. N. Bondarenko, and V. S. Zhigalov, JETP Lett. **88**, 515 (2008), V. S. Zhigalov, V. G. Myagkov, O. A. Bayukov, L. E. Bykova, G. N. Bondarenko, and A. A. Matsynin, JETP Lett. **89**, 621 (2009).

27. R. T. Lechner, V. Holÿ, S. Ahlers, D. Bougeard, J. Stangl, A. Trampert, A. Navarro-Quezada, and G. Bauer, Appl. Phys. Lett. **95**, 023102 (2009); F. Xiu, Y. Wang, K. Wong, Y. Zhou, X. Kou, J. Zou, and K. L. Wang, Nanotechnology **21**, 255602 (2010); A. Jain, M. Jamet, A. Barski, T. Devillers, I.-S. Yu, C. Porret, P. Bayle-Guillemaud, V. Favre-Nicolin, S. Gambarelli, V. Maurel, G. Desfonds, J. F. Jacquot, and S. Tardif, J. Appl. Phys. **109**, 013911 (2011); S. Yada, P. N. Hai, S. Sugahara, and M. Tanaka, J. Appl. Phys. **110**, 073903 (2011).

28. V. G. Myagkov, V. S. Zhigalov, A. A. Matsynin, L. E. Bykova, Yu. L. Mikhlin, G. N. Bondarenko, G. S. Patrin, and G. Yu. Yurkin, Thin Solid Films **552**, 86 (2014); V. G. Myagkov, V. S. Zhigalov, A. A. Matsynin, L. E. Bykova, G. V. Bondarenko, G. N. Bondarenko, G. S. Patrin, and D. A. Velikanov, JETP Lett. **96**, 40 (2012).

Translated by R. Tyapaev